Theoret. chim. Acta (Berl.) 20, 352—363 (1971)

Multi-Conformational Compounds with Two Absorbing Groups

V. The MIM Approach to α-Diketones*

AMATZYA Y. MEYER and YONIT KESTEN
Department of Organic Chemistry, Hebrew University, Jerusalem

Received September 28, 1970

The series of rotational isomers, derivable from α-diketones, has been studied by a "molecules-in-molecules" technique, including several diexcited configurations. Correlations concerning ground state properties and the dependence of spectral features upon conformation, are presented.

Die Reihe von Rotationsisomeren, die sich von α-Diketonen ableitet, wurde mittels des molecules-in-molecule Verfahrens untersucht, wobei zweifach angeregte Konfigurationen einbezogen wurden. Es interessierte besonders die Korrelation zwischen Eigenschaften des Grundzustandes und der Änderung der Spektren mit der Konformation.

On étudie les isomères rotationnels du système α-dionique par une méthode du type «molécules dans les molécules». Des configurations à excitation double sont incluses. Les calculs permettent d'établir des corrélations concernant l'état fondamental et la dépendence des spectres sur la conformation.

1. Introduction

In the preceding papers of this series [1], we analyzed the electronic properties of some non-planar monoketonic systems in terms of π-electron and all-valence-electron schemes. Extension of the analysis to compounds containing two carbonyl groups calls for a preliminary choice between the SCF-CI and MIM ("molecules-in-molecules" [2]) methods, and also for a decision as to the number and type of configurations to be included. We found it therefore desirable to develop the method step by step, increasing gradually the complexity of the model.

In the present paper we shall discuss the interdependence of rotational isomerism and electronic properties in α-diketones on the basis of a MIM construction.

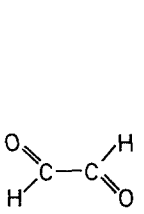

I

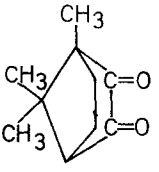

II

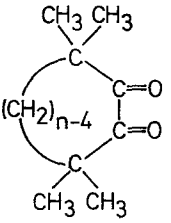

III

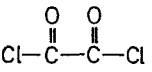

IV

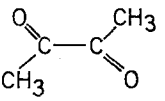

V

* For part IV, see Ref. [1].

Table 1

n	λ_{max} (nm) and ε[a, b]		Separation (eV)
5[c]	508 (38)	280 (15)	1.987
6	380 (11.1)	297.5 (28.9)	0.905
7	337 (33.8)	299 (34.5)	0.467
8	343 (21.4)	295.5 (43.2)	0.582
18	384 (21.7)	296 (50.6)	0.960

[a] Taken from Ref. [6], except $n = 5$.
[b] In 95% ethanol, except $n = 5$.
[c] In cyclohexane; Ref. [7].

We shall first consider the geometrical diversity of the α-diketones, in order to illustrate the need for a generalized treatment. Glyoxal (I) is known [3, 4] to adopt C_{2h}-symmetry, while the two carbonyl groups in camphorquinone (II) and its analogs [5] are necessarily *cis* to each other. The 3,3,*n*,*n*-tetramethyl-1,2-cyclanediones (III) show, in 95% ethanol, two $n \rightarrow \pi^*$ transition bands, whose position and intensity (Table 1) varies with n [6]. A logical assumption, corroborated by the spectral properties of other diones [8, 9], is that the change is related to modifications of the dihedral OCCO angle. In oxalyl chloride (IV), the dihedral angle is temperature-dependent. This follows [10] from the gas-phase spectrum which consists of a progression – with O–O band at 368 nm – superimposed on a continuum; the intensity of the former decreases, that of the latter increases with temperature. The 368 nm band is ascribed to the *trans*-, and the continuum – to a *cis*-rotamer.

The spectrum of glyoxal itself (I) has been measured both in the gas-phase [11] and in solution [12, 13]. The O–O band of the singlet $n \rightarrow \pi^*$ transition is found in the region 460–450 nm [3, 12, 14]. A progression at 320–230 nm, with a solution-maximum at 267.5 nm ($\varepsilon = 5.8$) [12], has been ascribed – by elimination – to a second $n \rightarrow \pi^*$ singlet [15]; however, the corresponding band of *biacetyl* (V) does not manifest the solvent-shifts expected for such a transition [16]. The next absorptions of glyoxal, at 205–185 nm (solution value 196 nm [12]) and at about 167 nm, were assigned [15] as $N \rightarrow B$ and $\pi \rightarrow \pi^*$, respectively.

Hückel-type calculations [17] apart, we know of six previous studies of glyoxal. In Sidman's evaluation of SCF π-orbitals [18], the oxygen non-bonding electrons were kept in the core. Other studies, with the *n*-orbital in the basis set, are the SCF–CI [19] and MIM [20] treatments of Edwards and Grinter, SCF–CI by Jensen and Skancke [21] and SCF by Leroy and Collab. [22]. All these calculations are limited, however, to C_{2h}-glyoxal, and it is not clear whether the proposed methods can be applied to other geometries or to long-chain carbon structures containing two carbonyl groups. All-valence-electron calculations for the *skew* glyoxal molecule have been performed by Hug and Wagnière [23]; here, however, the stress is laid upon optical activity, rather than the geometrical effect on π-electron properties.

We approach the geometrical problem by considering the unified α-diketone skeleton comprised of two carbonyl fragments, a and b (Fig. 1). The interatomic distances and bond angles are those of glyoxal [24], and the rotamers are identified

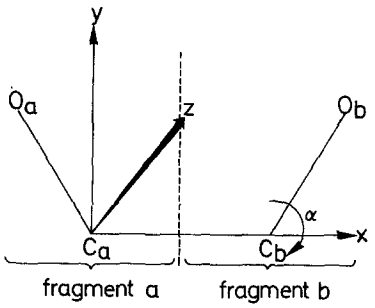

Fig. 1

by the angle α between the planes $OaCaC_b$ and $C_aC_bO_b$, such that $\alpha = 0°$ corresponds to the *cis*-structure. Each fragment contributes three $2p$-orbitals: χ_C and χ_O are π-orbitals and C and O, orthogonal to the lone-pair oxygen orbital, χ_n.

For each separate fragment, we begin with the three linear combinations

$$\pi = r\chi_C + s\chi_O ,$$
$$n = \chi_n ,$$
$$\pi^* = s\chi_C - r\chi_O ,$$

where r and s have the SCF values [25] of 0.5649 and 0.8251, respectively. We then construct the ground configuration,

$$G = (\pi_a\bar{\pi}_a n_a\bar{n}_a\pi_b\bar{\pi}_b n_b\bar{n}_b) ,$$
$$E_G \equiv 0 \quad \text{(for each separate rotamer)}$$

and twelve others, which fall into three categories.

1. Four local excitations (L): $n\pi^*(L, a)$, $n\pi^*(L, b)$, $\pi\pi^*(L, a)$, $\pi\pi^*(L, b)$, where a and b indicate the fragment, e.g.,

$$n\pi^*(L, a) = (1/\sqrt{2})\,(\pi_a\bar{\pi}_a[\pi_a^*\bar{n}_a + n_a\bar{\pi}_a^*]\,\pi_b\bar{\pi}_b n_b\bar{n}_b) .$$

2. Four charge-transfer excitations (CT): $\pi\pi^*(CT, a)$, $\pi\pi^*(CT, b)$, $n\pi^*(CT, a)$, $n\pi^*(CT, b)$, where a and b indicate the source of the transfer, e.g.,

$$\pi\pi^*(CT, a) = (1/\sqrt{2})\,([\pi_b^*\bar{\pi}_a + \pi_a\bar{\pi}_b^*]\,n_a\bar{n}_a\pi_b\bar{\pi}_b n_b\bar{n}_b) .$$

3. Four local diexcitations (D),

$$\pi\pi^*(D): \pi\pi^*(L, a) \text{ and } \pi\pi^*(L, b) ,$$
$$n\pi^*(D): n\pi^*(L, a) \text{ and } n\pi^*(L, b) ,$$
$$n\pi\pi^*(D): n\pi^*(L, a) \text{ and } \pi\pi^*(L, b) ,$$
$$\pi n\pi^*(D): \pi\pi^*(L, a) \text{ and } n\pi^*(L, b) .$$

Double excitations of the charge-transfer type were not included.

Formulation of the interaction matrix, with elements expressed first as sums of molecular [26], then of atomic integrals, and evaluation of these for each α and diagonalization furnish the desired state-energies and state-functions.

The evaluation of bicentric integrals over non-parallel atomic orbitals has been detailed elsewhere [1, 25, 27], and only an outline will be given here. An internal coordinate system is first constructed for each pair of orbitals, excepting pairs of parallel or perpendicular axes. Using the projections of the orbitals on the internal systems, one then reduces all bicentric integrals to sums of magnitudes which depend solely upon the interatomic distance. Coulomb repulsion integrals are obtained in terms of $(\sigma\sigma, \sigma\sigma)$, $(\pi\pi, \pi\pi)$, $(\pi\pi, \pi'\pi')$, $(\pi\pi, \sigma\sigma)$, $(\pi\pi', \pi\pi')$ and $(\pi\sigma, \pi\sigma)$ (where $\pi' \perp \pi$), and these are computed from Roothaan's formulas [28], with the effective exponents [25] 0.927 for C, 1.283 for O. Monoelectronic integrals are expressed as

$$\beta_{\mu\nu} = -k_{\mu\nu} S_{\mu\nu}$$

where we put $k_{CC} = 10.14$, $k_{CO} = 15.07$ and also derive $k_C = (1/2)\, k_{CC}$, $k_O = k_{CO} - k_C$, $k_{OO} = 2k_O = 20$.

The necessary overlap integrals, developed in terms of $S_{\pi\pi}$ and $S_{\sigma\sigma}$, are computed according to Mulliken *et al.* [29], with the Slater exponents 1.625 for C, 2.275 for O. Dipole moment integrals are evaluated as before [27].

The monocentric monoelectronic integral [1] follows immediately. The inclusion of a "π-inductive" correction for the pair O···C [cf. 21] caused only negligible modifications of the computed results, in distinction from our former findings concerning the F···C pair.

We adopt the ZDO approximation [30], which eliminates all bielectronic integrals except $(\mu\mu, \mu\mu)$, $(\chi_0\chi_n, \chi_n\chi_0) = (\pi\pi', \pi'\pi)_0$ and $(\mu\mu, \nu\nu)$. For the partial re-introduction of differential overlap (see later), we use [31]

$$(\mu\nu, \varrho\sigma) = (1/4)\, S_{\mu\nu} S_{\varrho\sigma} \sum_{\substack{\omega = \mu,\, \nu \\ \omega' = \varrho,\, \sigma}} (\omega\omega, \omega'\omega') .$$

Since it is our aim to obtain general relationships for widely differing diketones, not computed quantities for individual molecules, no parameter-optimization [cf. 20], nor use of empirical data [cf. 32] have been made.

2. Results and Discussion

A. General

Of the 78 interaction elements that occur in the 13×13 CI matrix, 46 vanish identically. Still, the matrix cannot be subdivided into independent blocks, as the other elements are in general interconnected. In particular, the diexcited configurations exert an α-dependent effect on the monoexcited levels, although only $n\pi^*$(D) is energetically comparable with them.

The ground-state, which contains about 97% of G at rotational extremes[1] and more than 99% mid-way, is depressed to the amount of 0.296 eV at 0°, 0.119 at 90° and 0.315 eV at 180°. These values, although suggestive, cannot be linked directly with the *trans*-geometry of glyoxal [3] as long as the compression-energies are not known [cf. 33]. Calculated ionization potentials exceed the

[1] Because of the need, dictated by the geometrical construction [27], for a special algorithm whenever $\sin \alpha = 0$, we have approximated 0° and 180° by 1′ and 179°59′, respectively.

Table 2. *Electronic states at* $\alpha \approx 0°$

State	Eigenvalue (eV)	Transition Wavelength (nm)	C_{2v} Representation[a]	f and Polarization[b]	Main Contributors
13	−0.2961	—	A_1	—	G
12	3.5000	326	A_2	$2 \cdot 10^{-6}\,(z)$	$n\pi^*$(L, −)
11	3.6361	315	B_2	$10^{-7}\,(z)$	$n\pi^*$(L, +)
10	7.6006	157	A_1	0.	$n\pi^*$(D)
9	7.6800	155	B_1	$0.186\,(xy)$	$\pi\pi^*$(L, −; CT, −)
8	7.9699	150	A_1	$0.553\,(yx)$	$\pi\pi^*$(L, +)
7	8.2700	144	B_2	$5 \cdot 10^{-5}\,(z)$	$n\pi^*$(CT, +)
6	8.4125	142	A_2	$10^{-4}\,(z)$	$n\pi^*$(CT, −)
5	10.6194	113	A_1	$0.021\,(xy)$	$\pi\pi^*$(CT, +)
4	11.9382	101	B_1	$8 \cdot 10^{-4}\,(xy)$	$\pi\pi^*$(L, −; CT, −)

[a] $C_2 \equiv y$, $\sigma_v \equiv xy$.
[b] See text.

Table 3. *Electronic states at* $\alpha = 90°$

State	Eigenvalue (eV)	Transition Wavelength (nm)	C_2 Representation[a]	f	Main Contributors
13	−0.1188	—	A	—	G
12	3.9056	308	B	10^{-7}	$n\pi^*$(L, −)
11	3.9056	308	A	$5 \cdot 10^{-7}$	$n\pi^*$(L, +)
10	7.2977	167	A	$3 \cdot 10^{-3}$	$n\pi^*$(D)
9	7.7024	158	A	0.231	$\pi\pi^*$(L, +)
8	8.3850	145	B	0.085	$n\pi^*$(CT, −)
7	8.6477	141	A	0.032	$n\pi^*$(CT, +)
6	9.5903	127	B	0.371	$\pi\pi^*$(L, −)
5	10.7123	114	A	$3 \cdot 10^{-5}$	$\pi\pi^*$(CT, +)
4	10.7124	114	B	$2 \cdot 10^{-4}$	$\pi\pi^*$(CT, −)

[a] C_2 bissects $O_a C_a C_b O_b$.

Table 4. *Electronic states at* $\alpha \approx 180°$

State	Eigenvalue (eV)	Transition Wavelength (nm)	C_{2h} Representation[a]	f and Polarization[b]	Main Contributors
13	−0.3148	—	A_g	—	G
12	3.6109	316	A_u	$5 \cdot 10^{-7}\,(z)$	$n\pi^*$(L, a)
11	3.6263	314	A_u	$10^{-6}\,(z)$	$n\pi$(L, b)
10	7.5756	157	A_g	0.	$n\pi^*$(D)
9	7.7123	154	A_g	$0.022\,(xy)$	$\pi\pi^*$(L, +)
8	7.9607	149	B_u	$0.623\,(yx)$	$\pi\pi^*$(L, −; CT, −)
7	8.5754	139	A_u	$10^{-4}\,(z)$	$n\pi^*$(CT, b)
6	8.6652	138	A_u	$4 \cdot 10^{-5}\,(z)$	$n\pi^*$(CT, a)
5	10.7832	111	A_g	$0.016\,(xy)$	$\pi\pi^*$(CT, +)

[a] $z \in A_u$; $x, y, \in B_u$.
[b] See text.

experimental glyoxal values [34], but the difference $I_\pi - I_n$, 3.59 eV at 180°, is exactly the same; at 0° and 90° one calculates 3.53 and 2.62 eV, respectively. Computed electroaffinities (depression included) are −1.98 at 0°, −0.93 at 90°, −2.02 eV at 180°, thus negative and close to the parameter-fitting value of −2.2 eV [20].

The properties of higher levels, and of transitions from the ground-state, are displayed in Tables 2–4 for the three rotational angles, 1′, 90° and 179°59′. Disregarding non-equal weighting, we denote symmetric and antisymmetric combinations by the (+) and (−) sign, respectively. Obviously, the symmetry connotation in Tables 2 and 4 refers to planar conformations, not to 1′ and 179°59′; this explains the non-vanishing oscillator-strengths (f) for formally forbidden transitions, as well as the replacement, in some cases, of axis-, by plane-polarization. On the other hand, "overlap-forbidenness" [18, 35] may weaken symmetry-allowed transitions, as is the case for $n\pi^*$(L)-excitations at 90° and $A_g \rightarrow A_u$ transitions at about 180°.

The excited levels may be grouped in five bands: The first, identifiable as $n \rightarrow \pi^*$(L), includes also the diexcitation, disregarded in former studies. The relation of the second, strong $\pi \rightarrow \pi^*$(L), to the third, weak $n \rightarrow \pi^*$(CT), illustrates interchange of electronic levels, predictive of change in the outward appearance of the spectrum. These are followed by $\pi \rightarrow \pi^*$ charge transfer and by the diexcitation band (not included in the tables) which comprises $\pi\pi^*$(D) (eigenvalue 17.36–17.90, dependent on α), as well as $n\pi\pi^*$(D) and $\pi n\pi^*$(D) (12.29–13.08).

The effect of geometry upon the first two bands is analyzed in the next sections.

B. $n \rightarrow \pi^*$ Transitions

The experimental data of Table 1 permit two generalizations [6, 36]. The first concerns the separation of the two bands, seen to be maximal at small and large dihedral angles, minimal mid-way; the second refers to the wavelength of the low-frequency absorption, which shows a similar behaviour. Naturally, these

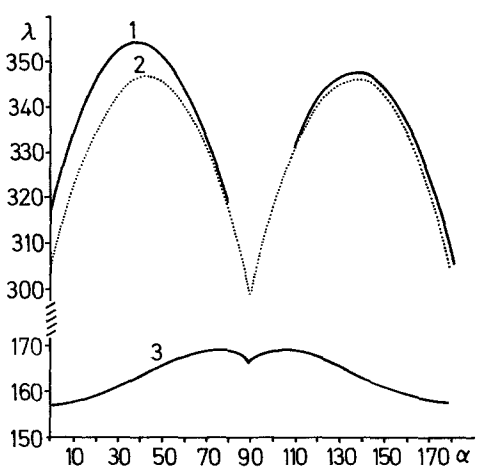

Fig. 2

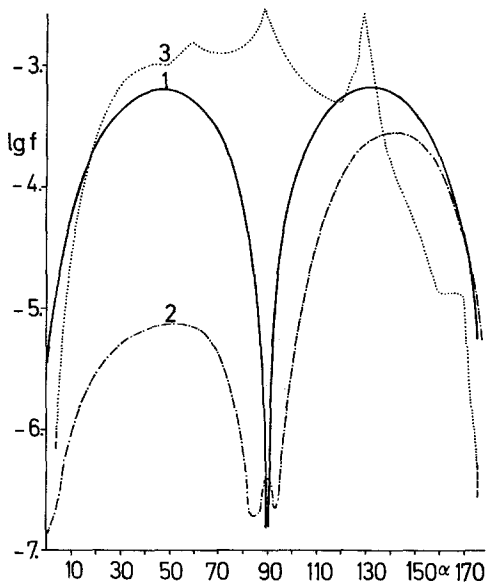

Fig. 3

relationships, derived from spectra of ethanol solutions, cannot be more than qualitative, because of the levelling effect [37] exerted on the shifted bands [38] in this hydroxylic solvent. A more fundamental reason to refrain from quantitative statements is that the numerical quantities depend strongly on the family of compounds, e.g., five-membered [36] and bicyclo-α-diketones [5] differ significantly from medium-ring [6] compounds.

Fig. 2 summarizes the angle-dependence computed for the two local $n \rightarrow \pi^*$ transitions (curves 1,2) and the corresponding diexcited state (curve 3); oscillator-strengths are shown in Fig. 3. The diexcitation, strictly forbidden at rotational extremes, has, at 90°, $M_x = 0.028$, $M_y = -0.039$, $M_z = -0.045$ (axes as in Fig. 1). The monoexcitations, weak but permitted throughout, are polarized as z: for the lower-energy band, $M_z = 0.0024$ at $\alpha = 0°$, $M_z = -0.0012$ at 180°, the values for the other being -0.0006 and -0.0021.

Suzuki has published [39] a schematic analysis, in terms of interacting molecular orbitals, both of the energy and of the separation of the two levels. It is of some interest to present the alternative MIM interpretation, supported by numerical quantities.

Under the limitations of the ZDO assumption, there can be no direct interaction between $n\pi^*(\mathrm{L}, a)$ and $n\pi^*(\mathrm{L}, b)$, nor between them and G. Indirect interaction exists, however, through the intermediary of the corresponding charge transfers, $n\pi^*(\mathrm{CT}, a)$ and $n\pi^*(\mathrm{CT}, b)$. True, $n\pi^*(\mathrm{L}, a)$ interacts with $\pi\pi^*(\mathrm{CT}, b)$ and $n\pi\pi^*(\mathrm{D})$, as does $n\pi^*(\mathrm{L}, b)$ with $\pi\pi^*(\mathrm{CT}, a)$ and $\pi n\pi^*(\mathrm{D})$, but this permits no "bridging", because

$$\langle [n\pi\pi^*(\mathrm{D})]\, \mathscr{H}\, [\pi n\pi^*(\mathrm{D})] \rangle \equiv 0\,,$$
$$\langle [\pi\pi^*(\mathrm{CT}, a)]\, \mathscr{H}\, [\pi\pi^*(\mathrm{CT}, b)] \rangle \equiv 0\,.$$

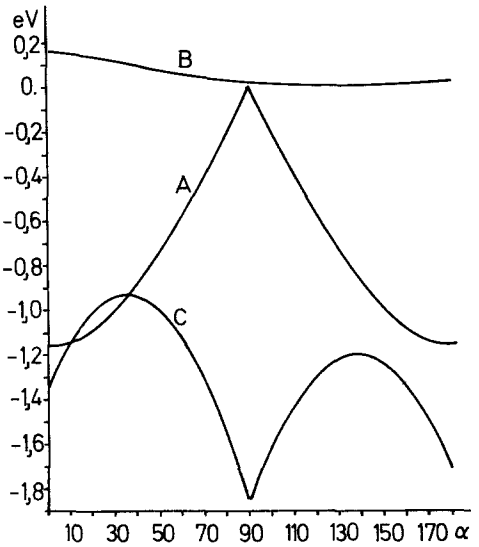

Fig. 4

The situation may be represented as

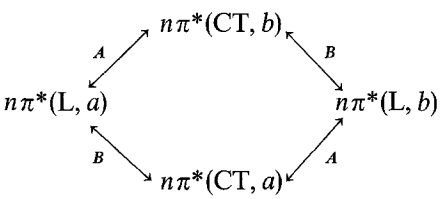

Element *A*, which links transitions of equal destination, depends essentially on the deviation of the molecule from planarity; symmetrically disposed about $\alpha = 90°$, it is highly negative (−1.15 eV) at 0° and 180°, zero at 90°. Element *B*, connecting transitions of equal source, is related mainly to the O···O distance; 0.16 eV at rotation 0°, it falls to 0.02 at 90°, diminishing further as one approaches the *trans*-rotamer. These relationships are shown in Fig. 4.

The separation of the two transitions is governed by the behaviour of *A* and *B*. In the first branch (0–90°), the separation is highest at 0° (*A* and *B* large in absolute value), nil at 90° ($A = 0$); going through the second (90–180°), it rises somewhat (*A* augments, but *B* diminishes), to fall again and vanish at 180° ($B \approx 0$).

The actual location of the $n \rightarrow \pi^*$ band is determined, first, by the energy of the $n\pi^*$(L) configurations before mixing, second, by the magnitude of the interaction-elements that push this energy *down*, towards the ground level. A third factor, namely, the ground-state depression, is numerically less important.

Before mixing, the $n \rightarrow \pi^*$ configurations are degenerate, with three energy-maxima, at 0°, and 90° and 180°. Upon mixing, the two states separate and their average energy, in respect to the ground-state, is lowered. The magnitude of this lowering has also three maxima, at 0°, 90° and 180°. One can then identify the

diexcited configurations $n\pi\pi^*$(D) and $\pi n\pi^*$(D) as responsible for this change, as their interaction-element with $n\pi^*$(L, *b*) and $n\pi^*$(L, *a*), respectively (curve *C* in Fig. 4), shows again the three maxima.

The importance of diexcited configurations, in calculations of this type, cannot be disregarded. In addition to the proximity of $n\pi^*$(D) and $\pi\pi^*$(L), noted above, we observe now that the lowering of $n\pi^*$(L), over-estimated before CI as 3.4–4.2 eV, is the numerical consequence of interaction with $n\pi\pi^*$(D) and $\pi n\pi^*$(D). The reduced values fall in the range 3.2–3.9 eV, still somewhat higher than some of the experimental data (see Sect. 1). Possibly, inclusion of additional *D*-type configurations, e.g., the "crossed" $n\rightarrow\pi^*$ charge-transfer, would have pushed the transition-energy even lower. This conclusion is independent of the ZDO assumption: partial re-introduction of differential overlap, rendering the element between $n\pi^*$(L, *a*) and $n\pi^*$(L, *b*) non-nul, was not found to influence the results significantly.

Turning next to the data of Table 1, a conformational analysis of the 3,3,*n*,*n*-tetramethyl-1,2-cyclanediones (III) can be attempted. Molecular models indicate [6] that, at $n=5$, the two carbonyl groups are confined to the *cis*-disposition, whereas an opening of the dihedral angle is possible for rings with larger *n*, and may amount to 100–180° at $n=18$. Obviously, the tendency to alleviate non-bonded interactions [6] is not the sole motivation for the dihedral opening, for glyoxal itself prefers *trans*-geometry. Assuming now that α augments with *n*, the level-separation data (Table 1), together with the trend of the first $n\rightarrow\pi^*$ absorption (Fig. 2), indicate $\alpha<90°$ for $n=6$, $\alpha>90°$ for $n=8$ and 18, α intermediate at $n=7$.

In order to narrow down the limits, we inspect the second $n\rightarrow\pi^*$ transition. Its wavelength is fairly constant in 95% ethanol; the molar extinction, on the other hand, is found to augment with *n*. Indeed, the data of Fig. 3 indicate that this quantity should increase with the dihedral angle, except in the intervals 60–100° and 140–180°. A possible interpretation is that $\alpha<60°$ for $n=6$ and 7, α between 100 and 140°– for $n=8$ and 18. A more precise analysis, however, cannot be based upon the reported data, because of the variety of effects [40] that determine solvent-shifts, and the ambiguity in the relation of theoretical *f* with ε_{max} and with [41] the experimental oscillator-strength.

C. $\pi\rightarrow\pi^*$ Transitions

Although less accessible to the practising organic chemist, it turns out that the $\pi\rightarrow\pi^*$ transitions should be even more revealing than the $n\rightarrow\pi^*$ bands. The two configurations, $\pi\pi^*$(L, *a*) and $\pi\pi^*$(L, *b*), lend themselves to two combinations, with angle-dependence as shown in Fig. 5. It is evident that, in distinction from the $n\rightarrow\pi^*$ bands, the two $\pi\rightarrow\pi^*$ absorptions have opposite trends, the one diminishing as the other augments. Disregarding edge-phenomena, there are two points of crossing, 74° and 107°, in the vicinity of which we find a double branching and four transitions, identifiable as $\pi\rightarrow\pi^*$.

The difference from $n\rightarrow\pi^*$ is based on the fact that $\pi\pi^*$(L, *a*) and $\pi\pi^*$(L, *b*) interact to a considerable extent, the interaction term changing sign at 10° (− to +), 74° (+ to −), 107° (− to +) and 163° (+ to −). Thus, the level separation, which

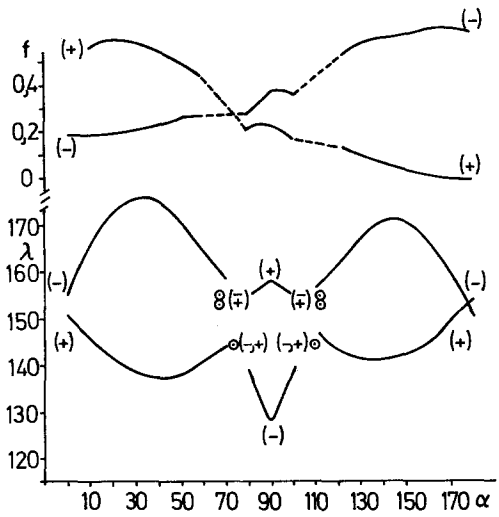

Fig. 5

amounts roughly to twice their interaction, vanishes twice along the rotational path (disregarding the edges), whereupon the crossing occurs.

It is in this context that the importance of the fourth diexcitation, $\pi\pi^*(D)$, becomes clear. The interaction $\langle[\pi\pi^*(L)]\mathscr{H}[\pi\pi^*(D)]\rangle$, which amounts to -1.151 eV at 0°, decreases monotonously to -1.371 at 180°, thus conveying to $\pi\pi^*(L)$ the effect of augmenting the O···O distance.

High oscillator-strengths, shown in Fig. 5, are the rule for local $\pi\rightarrow\pi^*$ transitions. In the coordinate-system of Fig. 1, one has

$$\left.\begin{aligned} M_x^- &= -0.513,\ M_y^- = 0.055 \\ M_x^+ &= 0.119,\ M_y^+ = -0.866 \end{aligned}\right\} \quad \text{at} \quad 0°,$$

$$\left.\begin{aligned} M_x^+ &= 0.133,\ M_y^+ = -0.398,\ M_z^+ = -0.401 \\ M_x^- &= -0.331,\ M_y^- = 0.403,\ M_z^- = -0.406 \end{aligned}\right\} \quad \text{at} \quad 90°,$$

$$\left.\begin{aligned} M_x^+ &= 0.163,\ M_y^+ = -0.075 \\ M_x^- &= -0.486,\ M_y^- = 0.790 \end{aligned}\right\} \quad \text{at} \quad 180°.$$

The high absorption coefficients, thus predicted, should be helpful in identifying $\pi\rightarrow\pi^*$ transitions, especially as they may be separated (Tables 2–4, Figs. 2 and 5) by $n\pi^*(D)$ and the two $n\pi^*(CT)$ combinations.

3. Summary

The interaction between two carbonyl groups, placed as in α-diketones, and the ensuing consequences for their properties, have been studied by a CI-model. As usual in such approaches, locally excited and charge-transfer configurations were included; in addition, it was shown that diexcitations are essential for reproducing the finer details.

The calculations lead to rationalization of experimental α-diketone properties, and also provide generalizations concerning the dependence of their spectra upon conformation. Yet, because of environmental effects, the theoretically-derived relationships should only be applied within series of related compounds.

The most remarkable characteristic of α-diketones is the separation of their two $n \rightarrow \pi^*$ absorptions. This is shown to be minimal in planar and perpendicular conformations, with a widening in-between. Regularities in the angle-dependence of wavelength and absorptivity were also formulated, and their utility was illustrated.

The $\pi \rightarrow \pi^*$ absorptions, although less accessible in routine work, are predicted to be even more indicative of steric relationships, because of marked separation and high oscillator-strength. The charge-transfer bands and diexcited levels, on the other hand, seem to be more useful as a technical tool than as a stereochemical probe.

References

1. Meyer, A. Y.: Theoret. chim. Acta (Berl.) **16**, 226 (1970).
2. Longuet-Higgins, H. C., Murrell, J. N.: Proc. physic. Soc. A **68**, 601 (1955).
3. Paldus, J., Ramsay, D. A.: Canad. J. Physics **45**, 1389 (1967).
4. Lu Valle, J. E., Schomaker, V.: J. Amer. chem. Soc. **61**, 3520 (1939).
5. Alder, K., Schäfer, H. K., Esser, H., Krieger, H., Reubke, R.: Ann. **593**, 23 (1955).
6. Leonard, N. J., Mader, P. M.: J. Amer. chem. Soc. **72**, 5388 (1950).
7. Sandris, C., Ourisson, G.: Bull. Soc. chim. France **1956**, 958.
8. Leonard, N. J., Blout, E. R.: J. Amer. chem. Soc. **72**, 484 (1950).
9. — Kresge, A. J., Oki, M.: J. Amer. chem. Soc. **77**, 5078 (1955).
10. Sidman, J. W.: J. Amer. chem. Soc. **78**, 1527 (1956).
11. Herzberg, G.: Molecular spectra and molecular structure, Vol. 3, p. 538. Princeton: Van Nostrand 1966.
12. Lüthy, A.: Z. Physik. Chem. **107**, 285 (1923).
13. Mackinney, G., Temmer, O.: J. Amer. chem. Soc. **70**, 3586 (1948).
14. Brand, J. C. D.: Trans. Faraday Soc. **50**, 431 (1954).
15. Walsh, A. D.: Trans. Faraday Soc. **42**, 66 (1946).
16. Forster, L. S.: J. Amer. chem. Soc. **77**, 1417 (1955).
17. Pullman, B., Pullman, A.: Les théories électroniques de la chimie organique. Paris: Masson 1952.
18. Sidman, J. W.: J. chem. Physics **27**, 429 (1957).
19. Edwards, T. G., Grinter, R.: Molecular Physics **15**, 357 (1968).
20. — — Theoret. chim. Acta (Berl.) **12**, 387 (1968).
21. Jensen, H., Skancke, P. N.: Acta chem. scand. **22**, 2899 (1968).
22. Aussems, C., Jaspers, S., Leroy, G., van Remoortere, F.: Bull. Soc. chim. Belgique **78**, 487 (1969).
23. Hug, W., Wagnière, G.: Theoret. chim. Acta (Berl.) **18**, 57 (1970).
24. Kuchitsu, K., Fukuyama, T., Morino, Y.: J. mol. Structure **1**, 463 (1968).
25. Meyer, A. Y., Serre, J.: Theoret. chim. Acta (Berl.) **8**, 117 (1967).
26. Slater, J. C.: Quantum theory of atomic structure, Vol. 1, p. 291. New York: McGraw-Hill 1960.
27. Meyer, A. Y.: J. Chim. physique **65**, 837 (1968).
28. Roothaan, C. C. J.: J. chem. Physics **19**, 1445 (1951).
29. Mulliken, R. S., Rieke, C. A., Orloff, D., Orloff, H.: J. chem. Physics **17**, 1248 (1949).
30. Fischer-Hjalmars, I.: Advances quant. Chem. **2**, 25 (1965).
31. Mulliken, R. S.: J. Chim. physique **46**, 500, 521 (1949).
32. Moscowitz, A., Hanssen, A. E., Forster, L. S., Rosenheck, K.: Biopolymers Symposia **1**, 75 (1964).
33. Nagakura, S.: Molecular Physics **3**, 105 (1960).
34. Turner, D. W.: cited in Ref. [20].

35. Sidman, J. W.: Chem. Rev. **58**, 689 (1958).
36. Sandris, C., Ourisson, G.: Bull. Soc. chim. France 350 (1958).
37. Kosower, E. M., Wu, G.-S.: J. Amer. chem. Soc. **83**, 3142 (1961).
38. Kasha, M.: Discuss. Faraday Soc. **9**, 15 (1950).
39. Suzuki, H.: Electronic absorption spectra and geometry of organic molecules, p. 434. New York: Academic Press 1967.
40. Bayliss, N. S., McRae, E. G.: J. physic. Chem. 58, 1002 (1954).
41. Allinger, N. L.: Tetrahedron **22**, 1367 (1966).

Dr. Amatzya Y. Meyer
Department of Organic Chemistry
Hebrew University
Jerusalem, Israel